

Sonoluminescence and collapse dynamics of multielectron bubbles in helium

J. Tempere,^{1,2} I. F. Silvera,² S. Rekhi,² and J. T. Devreese¹

¹*TFVS, Universiteit Antwerpen, Universiteitsplein 1, B2610 Antwerpen, Belgium*

²*Lyman Laboratory of Physics, Harvard University, Cambridge, Massachusetts*

(Dated: August 31, 2018)

Abstract

Multielectron bubbles (MEBs) differ from gas-filled bubbles in that it is the Coulomb repulsion of a nanometer thin layer of electrons that forces the bubble open rather than the pressure of an enclosed gas. We analyze the implosion of MEBs subjected to a pressure step, and find that despite the difference in the underlying processes the collapse dynamics is similar to that of gas-filled bubbles. When the MEB collapses, the electrons inside it undergo strong accelerations, leading to the emission of radiation. This type of sonoluminescence does not involve heating and ionisation of any gas inside the bubble. We investigate the conditions necessary to obtain sonoluminescence from multielectron bubbles and calculate the power spectrum of the emitted radiation.

I. INTRODUCTION

Multielectron bubbles (MEBs) are typically micron-sized cavities in liquid helium, containing a nanometer thin layer of electrons on the inside of the surface of the bubble. MEBs were first observed in experiments studying electrons on the surface of liquid helium beneath which an anode was present¹. When the charge density of the 2D-layer of electrons exceeds a critical value, a surface instability sets in² and a bubble forms, carrying up to 10^8 electrons to the anode. The electron system inside such a MEB is of particular interest, since it forms a spherical two-dimensional electron gas whose density can be tuned over a wide range of values depending on the number of electrons in the bubble and the pressure applied on the helium^{3,4}.

Unlike in gas-filled bubbles, the force preventing the bubble from imploding is not due to the pressure of a gas inside the bubble, but due to the Coulomb repulsion between the electrons in the MEB. At zero external pressure, the radius R_b of the bubble is determined by the balance between the Coulomb repulsion and the surface tension of the helium⁵. When the pressure p on the helium is nonzero, the bubble radius satisfies the equation

$$\frac{e^2 N^2}{4\pi\epsilon R_b^3} = 2pR_b + 4\sigma, \quad (1)$$

where e is the electron charge, N is the number of electrons in the MEB, ϵ is the dielectric constant of helium, and σ is the surface tension of helium. In the regime $pR_b/\sigma \gg 1$ the bubble radius scales as $p^{-1/4}$. In this paper we investigate what happens when a bubble with radius $R_b(p=0)$ in equilibrium at zero pressure is suddenly subjected to an increase in pressure. Its radius is larger than the equilibrium radius at pressure p , $R_b(p=0) > R_b(p)$ and we expect the bubble to shrink. In section II we derive and investigate the equations of motion for the bubble dynamics, and in section III we apply these equations to analyze the collapse dynamics of the multielectron bubble.

The fact that inside MEB's there are electrons (charged particles) instead of neutral gas atoms necessarily has another interesting consequence: the electrons in the compressing bubble are subject to accelerations, and therefore they generate electromagnetic radiation. The breathing mode of the bubble gives an estimate of the response time of the helium surface - which typically is microseconds for a 10000 electron MEB. In that time span, the bubble radius shrinks a distance of typically a micrometer. The velocity corresponding to this is of the order of micrometer/microsecond or m/s. But the acceleration this generates is

on the order of a micrometer/microsecond² which is quite large (10^6 m/s²). As the number of electrons increases, the initial bubble radius increases and the maximum acceleration increases as well. We will show that ultrashort light pulses can be produced by a sudden pressure increase in the helium surrounding the MEB.

Explanations of sonoluminescence in gas-filled bubbles^{6,7,8} have relied strongly on the emissivity of the heated gas in the collapsing gas-filled bubble¹⁰, as opposed to the mechanism of sonoluminescence proposed here for multielectron bubbles. Nevertheless gas-filled bubbles are known to get to temperatures where at least weak ionisation of the gas must occur⁸, and electrons can emit light, being accelerated through scattering from the neutral atoms. Although emission from accelerated electrons can contribute to the sonoluminescence of gas-filled bubbles⁹, it's precise role is still disputed¹⁰. For MEBs we propose that accelerating electrons form the principal mechanism of sonoluminescence. Moreover the light emission is expected to be coherent and coming from the bubble surface, whereas in gas-filled bubbles the emission is incoherent black-body emission from the interior of the bubble.

II. EQUATIONS OF MOTION FOR THE BUBBLE SURFACE

The bubble surface at time t can be described by the function $R(\theta, \phi, t)$ that gives the distance from the center of the bubble to the surface, in the direction specified by the spherical coordinates θ, ϕ . This function can be developed in spherical harmonics

$$R(\theta, \phi, t) = R_b(t) + \sum_{\ell=1}^{\infty} \sum_{m=-\ell}^{\ell} a_{\ell,m}(t) Y_{\ell,m}(\theta, \phi), \quad (2)$$

where R_b is the angle-averaged radius of the bubble. The coefficients $a_{\ell m}$ describe the deformation of the bubble from its spherical shape. To derive the equations of motion for the bubble surface, we start from the bubble Lagrangian derived in³:

$$\begin{aligned} \mathcal{L} = & 2\pi\rho R_b^3 \dot{R}_b^2 - \left(4\pi\sigma R_b^2 + \frac{4\pi}{3} p R_b^3 + \frac{e^2 N^2}{2\varepsilon R_b} \right) + \frac{\rho R_b^3}{2} \sum_{\ell,m} \frac{|\dot{a}_{\ell,m}|^2}{\ell+1} \\ & - \sum_{\ell,m} \left[\frac{\sigma}{2} (\ell^2 + \ell + 2) + p R_b - \frac{e^2 N^2}{8\pi\varepsilon R_b^3} \ell \right] |a_{\ell,m}|^2, \end{aligned} \quad (3)$$

where ρ represents the mass density of liquid helium. For small amplitude deformations of a spherical bubble, we know that $a_{\ell,m}(t) = a_{\ell,m}(0) \times \exp\{i\omega_\ell t\}$ where the ω_ℓ are the spherical

ripplon frequencies³. These frequencies can be obtained from (3) by putting $R_b(t) = R_{\text{eq}}$ where R_{eq} is the equilibrium radius:

$$\omega_\ell = \sqrt{\frac{\ell+1}{\rho R_{\text{eq}}^3} \left[\sigma(\ell^2 + \ell + 2) + 2pR_{\text{eq}} - \frac{e^2 N^2}{4\pi\epsilon R_{\text{eq}}^3} \ell \right]}. \quad (4)$$

In the Lagrangian (3), we have neglected the influence of the redistribution of the electrons along a deformed bubble surface. This effect can be described by introducing the (spherical) plasma oscillation modes of the electron system, and calculating the coupling between plasmons and ripples¹¹. In a recent study of this coupling Klimin *et al.*¹¹ found that although a bubble deformation does lead to a redistribution of charge along the surface, the resulting shift of the ripplon frequencies is small. The reason for the weakness of the ripplon-plasmon coupling is the difference in frequency of these modes: the ripplon frequencies typically lie in the MHz-GHz range, whereas the plasmon frequencies lie in the THz range.

The equation of motion for the radial component is

$$\frac{d}{dt} \frac{\partial \mathcal{L}}{\partial \dot{R}_b} = \frac{\partial \mathcal{L}}{\partial R_b}, \quad (5)$$

which yields

$$\begin{aligned} \frac{3}{2} \left(\frac{\dot{R}_b}{R_b} \right)^2 + \frac{\ddot{R}_b}{R_b} = & -\frac{1}{\rho R_b^4} \left(2\sigma R_b + pR_b^2 - \frac{e^2 N^2}{8\pi\epsilon R_b^2} \right) \\ & + \frac{3}{8\pi R_b^2} \sum_{\ell,m} \frac{|\dot{a}_{\ell,m}|^2}{\ell+1} - \frac{1}{4\pi\rho R_b^4} \sum_{\ell,m} \left[p - \frac{3e^2 N^2}{8\pi\epsilon R_b^4} \ell \right] |a_{\ell,m}|^2. \end{aligned} \quad (6)$$

The first line corresponds to the Rayleigh equation (with an additional electronic term) describing the collapse of spherical bubbles¹². The second line in (6) contains additional terms due to the deformation of the bubble.

The equation for the deformation components $\{a_{\ell,m}(t)\}$ is obtained from

$$\frac{d}{dt} \frac{\partial \mathcal{L}}{\partial \dot{a}_{\ell,m}^*} = \frac{\partial \mathcal{L}}{\partial a_{\ell,m}^*}, \quad (7)$$

which leads to

$$\ddot{a}_{\ell,m} + 3 \frac{\dot{R}_b}{R_b} \dot{a}_{\ell,m} = -\frac{\ell+1}{\rho R_b^3} \left[\sigma(\ell^2 + \ell + 2) + 2pR_b - \frac{e^2 N^2}{4\pi\epsilon R_b^3} \ell \right] a_{\ell,m}. \quad (8)$$

This equation is similar to the Plesset-Prosperetti equation¹³ in the theory of gas-filled bubbles in fluids. The set of equations (6) and (8) need to be solved given appropriate initial conditions.

Salomaa and Williams¹⁴ studied small-amplitude oscillations of multielectron bubbles using a similar set of equations. They neglected the contribution of the deformation amplitudes $\{a_{\ell,m}\}$'s in their equation for the radial component $R_b(t)$. This approximation is valid if $a_{\ell,m} \ll R_b$. They found that when the (time averaged) bubble radius satisfies $R_{\text{eq}} < [N^2 e^2 / (16\pi\sigma\varepsilon)]^{1/3}$, the $\ell = 2$ deformation can grow indefinitely, suggesting an instability of the bubble. In subsequent work³ it was found that the $\ell = 2$ ripplon frequency can indeed vanish, corroborating the results of Salomaa and Williams. However, an extension of ref.¹⁴ for large amplitude oscillation (i.e. beyond the regime $a_{\ell,m} \ll R_b$) showed that there exists a metastability barrier preventing the bubbles from fissioning¹⁵.

III. COLLAPSE OF A MULTIELECTRON BUBBLE

Having obtained the equations of motion for the bubble shape, we can proceed to solve them for the particular case of an MEB subjected to a sudden increase in pressure. We start with a bubble whose angle-averaged radius R_b is equal to the equilibrium radius $R_{\text{eq}}(p_0)$ at a given pressure p_0 of the liquid helium surrounding the MEB. This bubble can be either spherical ($\forall \ell, m : a_{\ell,m}(t=0) = 0$) or deformed ($\exists \ell, m : a_{\ell,m}(t=0) \neq 0$). At time $t = 0$ the pressure of the liquid helium jumps from p_0 to a higher value p . The angle-averaged radius is then larger than the equilibrium radius at pressure p and the bubble will collapse.

A. Spherical bubble

First we consider the collapse of an undeformed bubble. Then all $a_{\ell,m}$'s are zero and the dynamics are governed by the Rayleigh equation¹²

$$\frac{3}{2} \left(\frac{\dot{R}_b}{R_b} \right)^2 + \frac{\ddot{R}_b}{R_b} = -\frac{1}{\rho R_b^4} \left(2\sigma R_b + p R_b^2 - \frac{e^2 N^2}{8\pi\varepsilon R_b^2} \right), \quad (9)$$

in which an additional term due to the Coulomb repulsion of the electrons appears. This equation can be integrated once by multiplying left and right hand side by $2R_b^4 \dot{R}_b$, resulting in

$$\frac{d}{dt} \left(R_b^3 \dot{R}_b^2 \right) = -\frac{1}{2\pi\rho} \frac{d}{dt} \left[\left(\frac{e^2 N^2}{2\varepsilon R_b} + 4\pi\sigma R_b^2 + \frac{4\pi}{3} p R_b^3 \right) \right], \quad (10)$$

so that

$$\dot{R}_b^2 = -\frac{1}{2\pi\rho R_b^3} [U(R_b) - U(R_b(0))] \quad (11)$$

$$\text{where } U(R) = \frac{e^2 N^2}{2\varepsilon R} + 4\pi\sigma R^2 + \frac{4\pi}{3}pR^3. \quad (12)$$

This can again be integrated to yield

$$t(R) = \int_{R_b(0)}^R \left\{ \frac{1}{2\pi\rho r^3} [U(R_b(0)) - U(r)] \right\}^{-1/2} dr. \quad (13)$$

Note that the solution $R(t)$ is periodic, with the period given by $T = t(R_{\text{turn}})$ where R_{turn} is the classical turning point in the potential $U(r)$. In figure 1, the time evolution of the radius of a spherical $N = 10000$ electron bubble subjected to a sudden increase in pressure is shown. The top panel shows the pressure increase, and the subsequent panels show the radius, the radial velocity and the radial acceleration as a function of time divided by the period T . The initial conditions are $\dot{R}_b(0) = 0$ and $R_b(0) = 1.06441 \mu\text{m}$ - this corresponds to the $N = 10000$ electron bubble in equilibrium at zero pressure. The periods are $T = 0.795 \mu\text{s}$, $0.570 \mu\text{s}$ and $0.462 \mu\text{s}$ for pressure steps of 1, 2, and 3 kPa, respectively.

The radial acceleration shows a pronounced peak at the time when the MEB radius is minimal (the ‘time of collapse’). Upon increasing the pressure, the maximum radial acceleration grows and the oscillation of the radius becomes more strongly anharmonic. There is no dissipation term in our equation for the radius, so that the radius bounces back to its original value during the periodic oscillation. Dissipation will reduce this value and will let the bubble perform a damped oscillation around its new equilibrium radius $R_{\text{eq}}(p)$. As can be seen from figure 1, the time evolution of the radius of the MEB is very similar to that of a gas-filled bubble subjected to a shock wave⁶. In the latter case, the restoring force opposing the collapse is the increase in pressure of the gas trapped in the bubble. In the present case, the bubble contains no gas (except helium atoms at vapor pressure which is negligible at low temperatures), and it is the increased Coulomb repulsion that gives rise to the restoring force.

B. Deformed bubble

For small-amplitude deformations, $a_{\ell,m} \ll R_b$, we can neglect the $|a_{\ell,m}|^2$ terms in the equation (6) for the bubble radius, and use the solution for $R_b(t)$ discussed in the previous

section directly in the equation (8) for the deformation amplitudes. This equation can then be written as

$$\ddot{a}_{\ell,m}(t) + \lambda(t)\dot{a}_{\ell,m}(t) + \omega^2(t)a_{\ell,m}(t) = 0, \quad (14)$$

with the ‘drag coefficient’:

$$\lambda(t) = 3\dot{R}_b(t)/R_b(t), \quad (15)$$

and the time dependent ripplon frequency

$$\omega^2(t) = \frac{\ell + 1}{\rho R_b^3(t)} \left[\sigma(\ell^2 + \ell + 2) + 2pR_b(t) - \frac{e^2 N^2}{4\pi\epsilon R_b^3(t)} \ell \right]. \quad (16)$$

The time dependence of these coefficients (15),(16) appears through the time-dependence in R_b . The differential equation (14) can be solved numerically. The main question of this subsection concerns whether the deformations will vanish, grow without bound, or stay finite during the collapse of the bubble. From the numerical analysis we find that there are stable and unstable modes of deformation.

Note that even at a fixed pressure there are stable and unstable modes, as mentioned at the end of section II. Moreover, at higher pressure, more modes are unstable. When a pressure step Δp is applied, a mode that was stable at the initial pressure p_0 may be unstable at the final pressure $p_0 + \Delta p$.

An example of the time evolution of the amplitude of a stable mode is shown in figure 2. For this figure, we start with an $N = 10^4$ electron bubble at $p_0 = 0$ that has an $\ell = 25$ ripplon present. In this example, ℓ is chosen arbitrarily, but sufficiently high so that $\omega_\ell(p_0 + \Delta p) > 0$. Under the equilibrium conditions, the deformation amplitude oscillates with the corresponding ripplon frequency. When the pressure is suddenly increased by $\Delta p = 10^3$ Pa, we find that the oscillation perseveres, but that the oscillation amplitude is modulated with the same periodicity as the bubble radius. When the bubble radius is minimal, the oscillation amplitude of the deformation mode is maximal. This can be understood by substituting the ansatz $a_\ell(t) = A(t)e^{i\omega t}$ in the equation of motion (14). Collecting the imaginary parts of this equation, we arrive at

$$2\frac{\dot{A}(t)}{A(t)} + 3\frac{\dot{R}_b}{R_b} = 0, \quad (17)$$

from which

$$A(t) = CR_b^{-3/2}(t). \quad (18)$$

The constant of integration is given by $C = A(0)R_b^{3/2}(0)$. This solution is shown in figure 2 by the dashed curve. It fits well with the envelope of the full numerical solution (full curve), even though we started with a rather large deformation amplitude (10% of the radius) in order to get a clear figure. For stable modes, we thus find that during the collapse of a deformed bubble the deformations do not vanish. The deformation amplitude grows, but is bounded at all times.

An example of the time evolution of an unstable mode is shown in figure 3. As in figure 2 the initial state is that of an MEB with $N = 10^4$ electrons at pressure zero, subjected to a pressure increase of 10^3 Pa. The different curves in figure 3 represent different initial conditions, as listed in the legend. We chose the $\ell = 2$ mode because it is known to have a vanishing frequency at positive pressures and thus may lead to instabilities. The numerical solution of (14) shows that the deformation amplitude a_2 does indeed grow to a point where it becomes comparable to the bubble radius. This indicates that the collapsing MEB in helium becomes unstable and may break up, in contrast to gas-filled bubbles in cryogenic liquids¹⁶. Nevertheless, at the time of smallest radius, the deformation amplitude is still smaller than the bubble radius. The point of instability ($a_2 = R_b$) is reached after the collapse. So, although the bubble may not survive long after the first collapse, it will reach the regime where the radial acceleration is maximal one time. How long the bubble survives after it has reached its smallest radius, depends strongly on the initial conditions of the deformation. To study the exact dynamics of the instability (the possible fissioning), the full set of equations (6),(8) needs to be solved. This lies beyond the scope of this paper as we want to investigate the collapse dynamics and luminescence during collapse, but not the possible breaking up of bubbles during the explosion that follows after the implosion.

IV. LIGHT RADIATION FROM AN IMPLODING MEB

A. Incoherent emission from a spherical bubble

The electric radiation field by an accelerated charge is given by

$$\mathbf{E}(\mathbf{r}, \mathbf{R}, t) = \frac{q}{c^2} \frac{\mathbf{n} \times [\mathbf{n} \times \ddot{\mathbf{R}}(t)]}{|\mathbf{r} - \mathbf{R}(t)|} \bigg|_{\text{ret}}, \quad (19)$$

where $\mathbf{R}(t)$ gives the trajectory of the charge q , \mathbf{r} is the point in which we want to evaluate the electric radiation field, \mathbf{n} is the unit vector along $\mathbf{r} - \mathbf{R}(t)$, and c is the speed of light in vacuum. Note that there is a non-radiative part of the electric field (of order $[\mathbf{r} - \mathbf{R}(t)]^{-2}$ and higher). This is usually neglected at large distances from the accelerated electron. However, if the radiative field is cancelled, for example by symmetry considerations, then these higher order fields come into play so that the Maxwell equations remain satisfied. The subscript “ret” means that the electric field at time t is generated by the accelerating electron at a time t' earlier by the delay it takes the light to reach \mathbf{r} . In our situation, this retardation is of no consequence. From figure 2, it can be seen that though the radial velocity of the electrons is fairly high, it is not relativistic (the acceleration, be it large, only takes place in a very short time scale). The power radiated per unit of solid angle per electron is

$$\frac{dP}{d\Omega} = \frac{e^2}{4\pi c^3} |\mathbf{n} \times [\mathbf{n} \times \ddot{\mathbf{R}}]|^2 = \frac{e^2}{4\pi c^3} |\ddot{R}|^2 \sin^2 \theta, \quad (20)$$

with θ the angle between the direction of the acceleration and \mathbf{n} . Thus the maximum radiated power is

$$P = \frac{2Ne^2}{3c^3} |\ddot{R}|^2. \quad (21)$$

We first consider a light pulse that might be emitted by a single electron in an MEB. The light pulse intensity is peaked at the instant when the bubble reaches its smallest radius, stops imploding and starts expanding again. At this point, the radial acceleration $|\ddot{R}|$ is largest. This is similar to what happens in sonoluminescence in gas-filled bubbles. For bubbles with 10000 electrons, and a pressure step of 3 kPa, a pulse of roughly 50 ns is emitted, as can be seen from figure 1, bearing in mind that in that case $T = 0.462 \mu\text{s}$. Increasing the pressure step will shorten the length of the pulse, and increase the maximum acceleration reached (see figure 1). In figure 4 we show the width Δt_{pulse} at half maximum of the peak in the radial acceleration, as a function of pressure for different numbers of electrons. Large MEBs ($N = 10^7$), such as those created in the experiments reported in Refs.¹, have a very high compressibility resulting in ultrashort pulses and very large radial accelerations. Figure 5 shows the power as a function of time (and frequency, in the inset) for an extreme case: an $N = 10^7$ electron bubble subjected to a pressure step of 101.3 kPa. The ultrashort pulse reaches a maximum power of 100 μW (i.e. 10^{-11} W per electron). Of course, one can ask whether for such an extreme case, the equation of motion (9) remains valid up to the time

that the smallest radius is reached. If the surrounding helium is heated up by the radiation, or if the electrons penetrate into the helium, then the bubble implosion may have different dynamics. Nevertheless, it seems safe to expect that equation (6) remains valid for a large portion of the collapse, and that for not so extreme cases the qualitative results hold. These results are that if the number of electrons or the pressure step is increased, the pulse duration shortens, the emitted spectrum shifts to higher frequencies, and the maximum power of the pulse increases.

B. Sonoluminescence from deformed bubbles

The results of the previous subsection were for one accelerating electron, or for a collection of electrons emitting radiation incoherently. If the electric field of all the electrons is added coherently, then for an undeformed bubble the radiation of the collapsing shell of electrons will vanish due to the spherical symmetry, as we shall prove.

We investigate the case where one of the deformation amplitudes $a_{\ell,m}$ is nonzero. In studying modes of vibration where $m \neq 0$, the restriction $a_{\ell,-m} = a_{\ell,m}^*$ applies because the surface $R(\Omega, t)$ has to be described by a real function, and thus

$$\mathbf{R}(\Omega, t) = \{R_b(t) + 2 \operatorname{Re}[a_{\ell,m}(t)Y_{\ell,m}(\Omega)]\} \mathbf{n}_\Omega \quad (22)$$

$$= R_b(t) [1 + \tilde{a}_{\ell,m}(t)P_\ell^m(\cos \theta) \cos(m\phi)] \mathbf{n}_\Omega, \quad (23)$$

where P_ℓ^m is the associated Legendre function, \mathbf{n}_Ω is the unit vector normal to the surface and the rescaled deformation amplitude $\tilde{a}_{\ell,m}$ is given by

$$\tilde{a}_{\ell,m}(t) = 2 \frac{a_{\ell,m}(t)}{R_b(t)} \sqrt{\frac{2\ell+1}{4\pi} \frac{(\ell-m)!}{(\ell+m)!}}. \quad (24)$$

We evaluate the electric field at a point

$$\mathbf{r} = r (\mathbf{e}_x \sin \alpha \sin \beta + \mathbf{e}_y \sin \alpha \cos \beta + \mathbf{e}_z \cos \alpha), \quad (25)$$

where we assume that $r \gg R$, i.e. the radiation field is evaluated at a large distance from the bubble. Furthermore, we will assume that $\ddot{a}_{\ell,m} \ll \ddot{R}_b$, which is valid when the bubble is near its minimum radius, and when the initial deformation satisfies $a_{\ell,m}(t=0) \ll R_b(t=0)$.

Substitution of (23) in (19) results in

$$\mathbf{E}(r \gg R) \approx \frac{Ne}{c^2} \frac{\ddot{R}_b(t)}{r} \times \int d\Omega \left\{ \frac{R(\Omega, t)}{R_b(t)} \Theta(\Omega) \mathbf{e}_r - \frac{\mathbf{R}(\Omega, t)}{R_b(t)} \right\} \quad (26)$$

$$= \frac{Ne}{c^2} \frac{\ddot{R}_b(t)}{r R_b(t)} \times \int d\Omega [1 + \tilde{a}_{\ell, m}(t) P_\ell^m(\cos \theta) \cos(m\phi)] [\Theta(\theta, \phi) \mathbf{e}_r - \mathbf{e}_R], \quad (27)$$

where the angular function is given by

$$\Theta(\theta, \phi) = \cos \alpha \cos \theta + \sin \alpha \cos \beta \sin \theta \cos \phi + \sin \alpha \sin \beta \sin \theta \sin \phi. \quad (28)$$

The components of the electric field are, for $r \gg R$

$$\begin{pmatrix} E_x \\ E_y \\ E_z \end{pmatrix} \approx \frac{q}{c^2} \frac{\tilde{a}_{\ell, m}(t) \ddot{R}_b(t)}{r} \times \int_0^\pi d\theta \sin \theta P_\ell^m(\cos \theta) \int_0^{2\pi} d\phi \cos(m\phi) \\ \times \begin{pmatrix} \Theta(\theta, \phi) \sin \alpha \cos \beta - \sin \theta \cos \phi \\ \Theta(\theta, \phi) \sin \alpha \sin \beta - \sin \theta \sin \phi \\ \Theta(\theta, \phi) \cos \alpha - \cos \theta \end{pmatrix}. \quad (29)$$

From the integration over the ϕ coordinate, it is clear that only the $m = 0, \pm 1$ terms result in a nonzero radiation field. The integration over the θ angle finally yields

$$\begin{pmatrix} E_x \\ E_y \\ E_z \end{pmatrix} \approx \sqrt{\frac{4\pi}{3}} \frac{Ne}{c^2} \frac{\ddot{R}_b(t)}{r R_b(t)} \\ \times \begin{pmatrix} (\cos \alpha \sin \alpha \cos \beta) a_{1,0} + (1 - \sin^2 \alpha \cos^2 \beta) a_{1,1} \\ (\cos \alpha \sin \alpha \sin \beta) a_{1,0} - (\sin^2 \alpha \sin \beta \cos \beta) a_{1,1} \\ (\sin^2 \alpha) a_{1,0} - (\sin \alpha \cos \alpha \cos \beta) a_{1,1} \end{pmatrix}. \quad (30)$$

Note that only the $\ell = 1$ mode contributes to the radiation field. This proves our earlier statement that the radiation fields of electrons on an accelerating *spherical* shell cancel out.

The emitted power is then given by

$$P(\alpha, \beta) = N^2 P_0 \left[\begin{pmatrix} \sin \alpha \cos \beta \cos \alpha \\ \sin \alpha \sin \beta \cos \alpha \\ -\sin^2 \alpha \end{pmatrix} \frac{a_{1,0}}{R_b} - \begin{pmatrix} \sin^2 \alpha \cos^2 \beta - 1 \\ \sin^2 \alpha \cos \beta \sin \beta \\ \cos \alpha \sin \alpha \cos \beta \end{pmatrix} \frac{a_{1,1}}{R_b} \right]^2, \quad (31)$$

with $P_0 = (4\pi/3)e^2\ddot{R}_b^2/c^3$. Using typical values $N = 10^6$, $a_{\ell m} \approx 0.01 R_b$, $p_0 = 0$ and $\Delta p = 100$ kPa, we find a maximum power of the order of $100 \mu\text{W}$ (for a pulse length of the order of 10 fs). Although this may seem a lot, because of the short pulse time only a small amount of energy is emitted, corresponding to 10-100 photons with frequency $1/(10 \text{ fs})$. This will make the detection of the light difficult in practice. Photons of successive collapse-expansion cycles may be collected, but dissipation may quickly dampen the oscillations. If the bubble oscillations after a single pressure step dampen out quickly, repeating the pressure step using an ultrasonic wave of e.g. 1 KHz can increase the number of photons to be collected. Another possibility may be to work with larger bubbles since the total number of electrons affects very strongly the maximum peak power, through the coherency factor N^2 in (31) and the strong dependence of \ddot{R}_b on N . For example, a $N = 10^5$ electron bubble subjected to the same $\Delta p = 100$ kPa pressure step has a maximum peak power of $10^{-2} \mu\text{W}$ (for $a_{\ell m} \approx 0.1 R_b$). In the extreme case of large bubbles ($N > 10^7$) subjected to large pressure steps (Δp of the order of 10^5 Pa), the power radiated can become large enough to affect the collapse dynamics significantly, and expression (31) is no longer valid. Two factors will act to reduce the maximum power: incoherency effects (such as those caused by the finite time needed for a pressure wave to travel across the bubble) and the smallness of the deformations (typically, we assumed $a_{\ell m} \ll R_b$).

The last factor in (31) is the geometrical factor giving the angle-dependence of the radiation and relating its strength to the deformation amplitude. The collapsing deformed bubble will radiate anisotropically. Figure 6 shows the angular dependence of the radiated power. The $(\ell, m) = (1, 0)$ mode will emit most strongly in the equatorial plane of the bubble, whereas the $(\ell, m) = (1, \pm 1)$ modes will emit most strongly along meridians.

V. DISCUSSION AND CONCLUSION

When an MEB is subjected to a sudden increase in pressure $p_0 \rightarrow p_0 + \Delta p$, its radius is larger than the new equilibrium radius $R_{\text{eq}}(p_0) > R_{\text{eq}}(p_0 + \Delta p)$ and it shrinks to a final radius that is smaller than the new equilibrium radius $R_{\text{eq}}(p_0 + \Delta p)$, after which it expands again. This oscillatory motion of collapses and expansions occurs on a time scale of microseconds, but the oscillation becomes greatly anharmonic, in that most of the reduction in radius occurs in a small fraction of the total cycle. This leads to large accelerations when the

radius of the bubble is smallest. When deformations are present, the normal modes of deformation with a ripplon frequency larger than the inverse time scale of the collapse are stable. Modes with small ripplon frequencies (such as the $\ell = 2$ quadrupole oscillation modes) grow unbounded and can lead to instabilities and fissioning of the collapsing bubble. However, we find that at the time when the bubble has reached its smallest radius, and the radial acceleration is maximal, the deformation mode is not yet diverging. This conclusion is important for the possibility to observe sonoluminescence of the collapsing MEBs. In a purely spherical bubble, coherent emission of radiation by the accelerated electrons cancel out due to symmetry requirements. Thus, to produce a radiation field, the collapsing bubble should be deformed. We find that in a collapsing bubble where the $\ell = 1$ mode of deformation is present, the radiation fields of the electrons do not cancel. One might wonder how this particular mode can be excited so that sonoluminescence can be generated in an experiment. It turns out that it is not necessary to artificially excite this mode: Plesset¹³ showed that gas-filled bubbles that implode near a surface naturally develop a deformation corresponding exactly to the $\ell = 1$ mode, and we expect that this surface proximity effect will also be present for imploding multielectron bubbles.

In the derivation, it was assumed that the temperature is low enough so that the vapor pressure of helium inside the MEB is negligible. It is worth noting that if helium vapor is present inside the bubble, the pressure of this vapor will increase as the bubble collapses and a mist of helium may be formed that can affect the dynamics of the bubble collapse¹⁷.

In summary, we have investigated the dynamics of collapsing multielectron bubbles in liquid helium and the possibility that imploding MEBs emit radiation. We find that these bubbles behave in a similar manner as gas-filled bubbles, even though the fundamental mechanism involved in the bubble dynamics is different. In MEBs the force counteracting the collapse bubble is Coulomb repulsion, whereas in gas-filled bubbles this force is due to the gas pressure inside the bubble. The collapse of a MEB subjected to a pressure step leads to the emission of radiation due to the acceleration of the shell of electrons at the bubble surface, whereas sonoluminescence in gas-filled bubbles is due to a more complex combined effect of heated gas emissivity and bremsstrahlung.

Acknowledgement 1 *Discussions with D. Lohse are gratefully acknowledged. J. T. is supported financially by the FWO-Flanders. This research has been supported by the Department*

of Energy, Grant DE-FG02-ER45978, and by the GOA BOF UA 2000, NOI BOF UA 2004, IUAP, the FWO-V projects Nos. G.0435.03, G.0274.01, G.0306.00.

-
- ¹ A.P. Volodin, M.S. Khaikin, and V.S. Edelman, Pis'ma Zh. Eksp. Teor. Fiz. **26**, 707 (1977) [JETP Lett. **26**, 543 (1977)]; U. Albrecht and P. Leiderer, Europhys. Lett. **3**, 705 (1987).
 - ² L.P. Gor'kov and D.M. Chernikova, Pis'ma Zh. Eksp. Teor. Fiz. **18**, 119 (1973) [JETP Lett. **18**, 68 (1973)].
 - ³ J. Tempere, I. F. Silvera, J. T. Devreese, Phys. Rev. Lett. **87**, 275301 (2001)
 - ⁴ J. Tempere, S. N. Klimin, I. F. Silvera, J. T. Devreese, European Physical Journal B **32**, 329 (2003).
 - ⁵ V.B. Shikin, Pis'ma Zh. Eksp. Teor. Fiz. **27**, 39 (1978) [JETP Lett. **27**, 39 (1978)].
 - ⁶ D. F. Gaitan, Ph.D. Thesis, University of Mississippi, 1990 (unpublished); D. F. Gaitan, L. A. Crum, R. A. Roy, and C. C. Church, J. Acoust. Soc. Am. **91**, 3166 (1992).
 - ⁷ R. Hiller, S. J. Putterman, and B. P. Barber, Phys. Rev. Lett. **69**, 1182-1184 (1992).
 - ⁸ M. P. Brenner, S. Hilgenfeldt, and D. Lohse, Rev. Mod. Phys. **74**, 425-484 (2002).
 - ⁹ D. Hammer and L. Frommhold, J. Mod. Opt. **48**, 239 (2001).
 - ¹⁰ S. Hilgenfeldt, S. Grossmanm, and D. Lohse, Nature **398**, 402 (1999).
 - ¹¹ S. N. Klimin, V. M. Fomin, J. Tempere, I. F. Silvera and J. T. Devreese, Solid State Commun. **126**, 409 (2003).
 - ¹² Lord Rayleigh, Philos. Mag. **34**, 94 (1917).
 - ¹³ M. S. Plesset and A. Prosperetti, Ann. Rev. Fluid Mech. **9**, 145 (1977).
 - ¹⁴ M. M. Salomaa and G. A. Williams, Phys. Rev. Lett. **47**, 1730 (1981).
 - ¹⁵ J. Tempere, I. F. Silvera, and J. T. Devreese, Phys. Rev. B **67**, 035402 (2003).
 - ¹⁶ O. Baghdassarian, B. Tabbert, and G.A. Williams, Physica B **284-288**, 393 (2000).
 - ¹⁷ F. Takemura and Y. Matsumoto, JSME International Journal Series B - Fluids and Thermal Engeneering **37**, 736 (1994); K. Yasui, Phys. Rev. E **58**, 471 (1998).

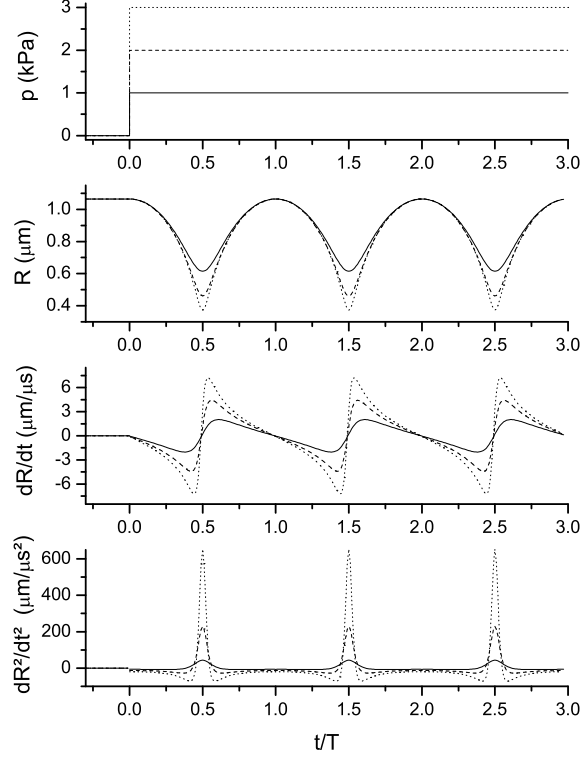


FIG. 1: A multielectron bubble with $N = 10^4$ electrons at zero external pressure, is subjected at time $t = 0$ to a pressure increase of $\Delta p = 1, 2, 3$ kPa (full, dashed and dotted curves, respectively). In this figure, the panels from top to bottom show the pressure, the bubble radius, the radial velocity and the radial acceleration as a function of time. All these quantities are cyclic with period $T = 0.795 \mu\text{s}$, $0.570 \mu\text{s}$ and $0.462 \mu\text{s}$ for pressure steps of 1, 2, and 3 kPa, respectively.

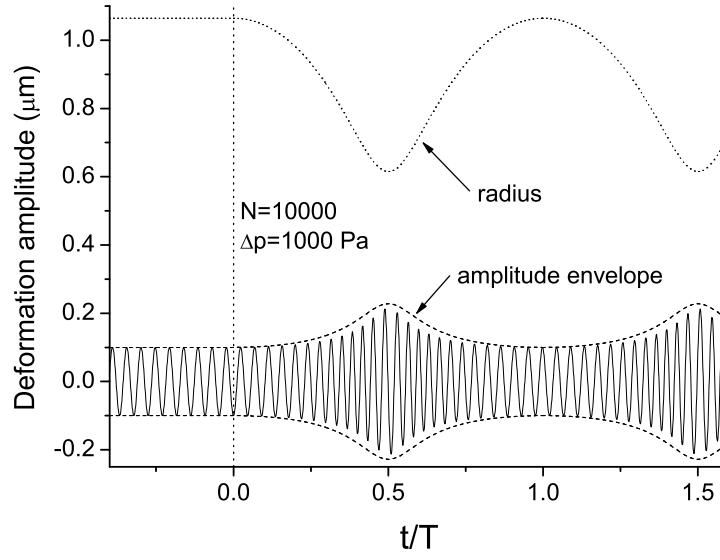


FIG. 2: The time evolution of the amplitude of deformation associated with the $\ell = 25$ ripplon is shown (full curve) for an $N = 10^4$ electron bubble subjected to a pressure increase of 1 kPa at time $t = 0$. The dashed curve shows the analytical estimate for the the envelope of the oscillating deformation amplitude. The dotted curve depicts the radius of the bubble.

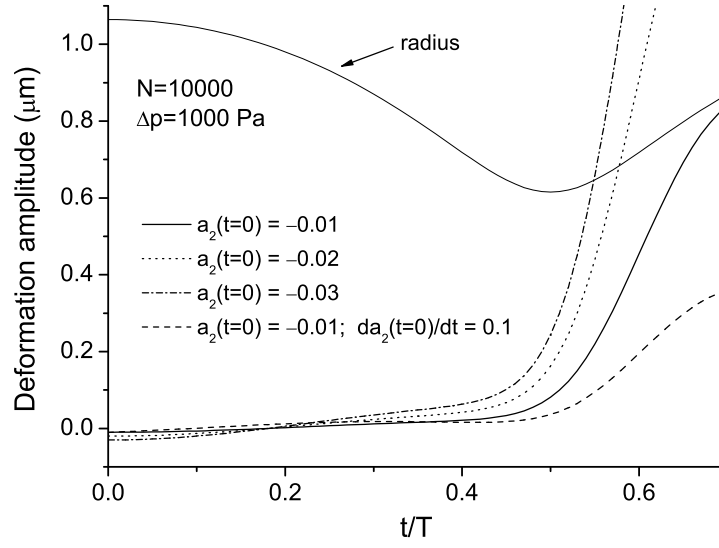


FIG. 3: The time evolution of an unstable ($\ell = 2$) mode of an $N = 10^4$ bubble subjected to a pressure increase of $p = 10^3$ kPa. The deformation amplitude grows larger than the bubble radius (so that the bubble is unstable) some time after collapse (i.e. after the bubble radius reaches its minimum), depending on the initial conditions.

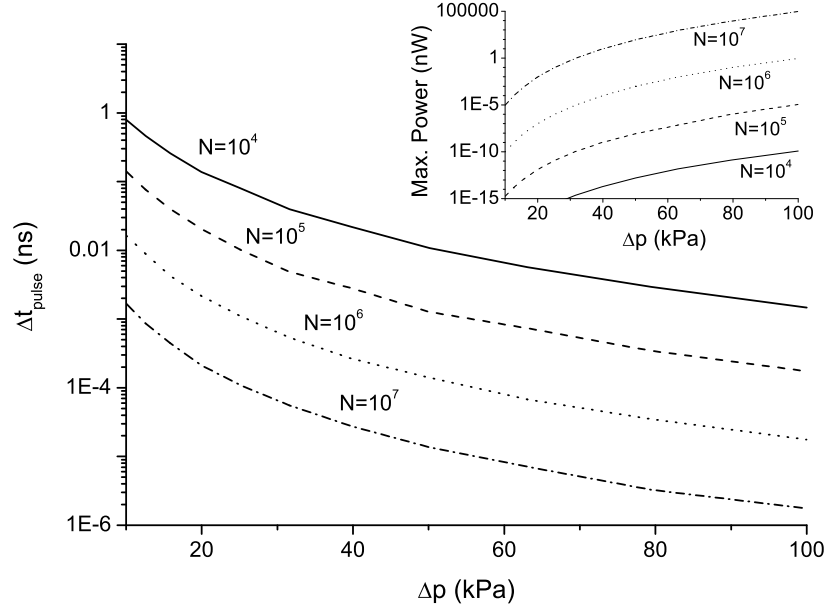


FIG. 4: The width at half maximum Δt_{pulse} of the peak in the radial acceleration of the collapsing bubble as it reaches its smallest radius is shown as a function of the pressure step causing the collapse, for different values of the number of electrons in the MEB. In the inset, the maximum power of the emitted radiation pulse is shown as a function of the pressure step and the number of electrons.

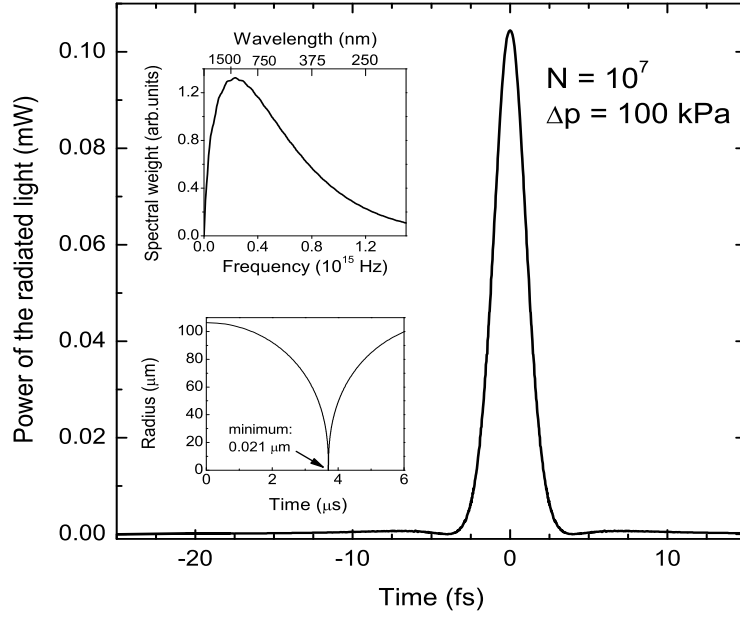


FIG. 5: For very large MEBs (10^7 electrons) subjected to a large pressure step (100 kPa), the emitted pulse of radiation calculated with (6),(19) can become extremely short and reach 100 μW peak power. This also results in a broad spectrum of the emitted radiation, as shown in the upper inset. The lower inset shows the bubble radius as a function of time (cf fig. 1).

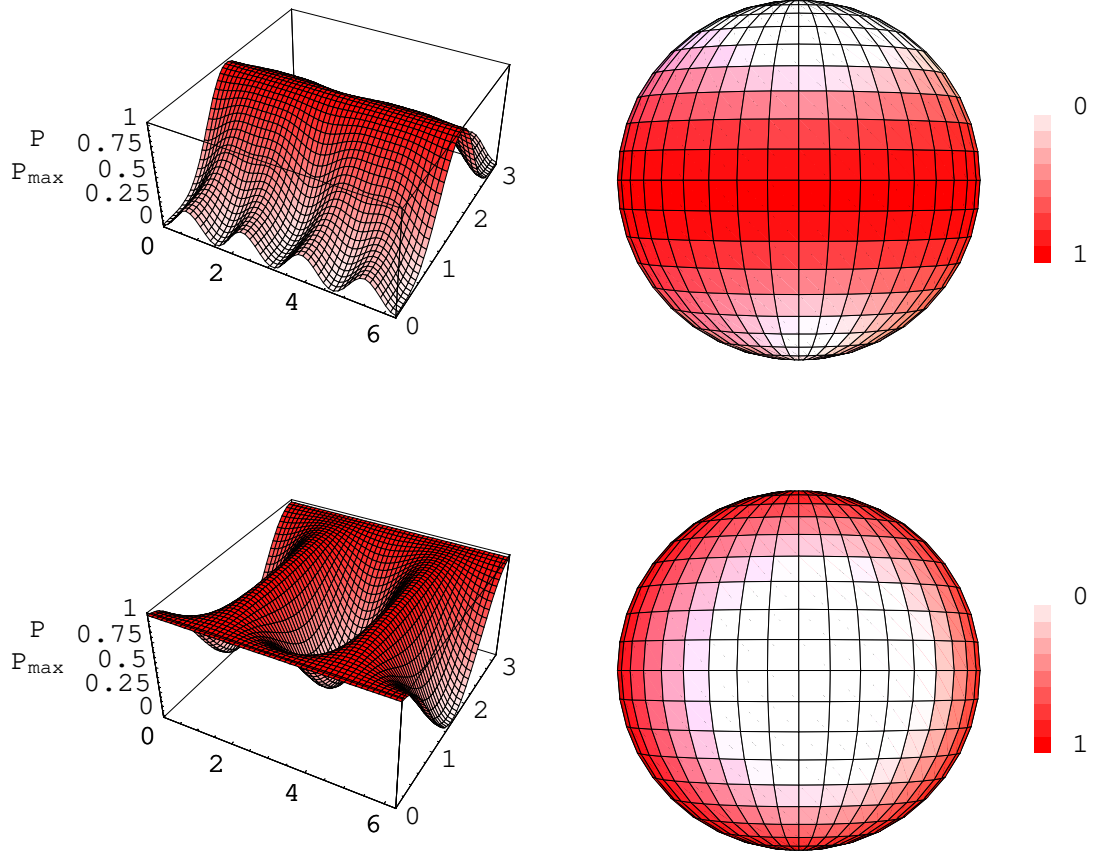


FIG. 6: The maximum power (expression (31)) of the radiation from a collapsing deformed bubble is shown as a function of the spherical angles θ and ϕ . The power is expressed relative to maximum power as a function of the angles. The top two figures are for the $a_{1,0} \neq 0, a_{1,1} = 0$ case and the bottom two figures for the $a_{1,0} = 0, a_{1,1} \neq 0$ case. The illustrations on the right show the regions on the sphere (with the z -axis in the vertical direction) where radiation is emitted (shaded regions) in both cases.